Thermochimica Acta 478 (2008) 45–50

Contents lists available at ScienceDirect

Thermochimica Acta

journal homepage: www.elsevier.com/locate/tca

Studies on the oxidation properties of nanopowder CeO_2-based solid solution catalysts for model soot combustion

Ping Fang[a,b], Meng-Fei Luo[a,*], Ji-Qing Lu[a], Shu-Qiong Cen[a,b], Xin-Yu Yan[a], Xiao-Xia Wang[a]

[a] Zhejiang Key Laboratory for Reactive Chemistry on Solid Surfaces, Institute of Physical Chemistry, Zhejiang Normal University, Jinhua 321004, China
[b] Analysis and Measurements Research Center, Shaoxing University, Shaoxing 312000, China

ARTICLE INFO

Article history:
Received 6 March 2008
Received in revised form 3 July 2008
Accepted 29 August 2008
Available online 11 September 2008

Keywords:
CeO_2-based solid solutions
Oxygen vacancies
Soot combustion
Catalytic activity

ABSTRACT

The catalytic behavior of CeO_2-based solid solution catalysts ($Ce_{0.7}Zr_{0.3}O_2$, $Ce_{0.7}Pr_{0.3}O_{2-\delta}$, and $Ce_{0.7}Gd_{0.3}O_{1.85}$) had been studied for soot combustion. These catalysts were characterized using X-ray diffraction (XRD), UV-visible, Raman, and H_2 temperature-programmed reduction (H_2-TPR) measurements. The Zr, Pr, and Gd cations replaced Ce cations in the CeO_2 lattice to form nanocrystalline CeO_2-based solid solutions. The crystallite size of $Ce_{0.7}Zr_{0.3}O_2$, $Ce_{0.7}Pr_{0.3}O_{2-\delta}$, and $Ce_{0.7}Gd_{0.3}O_{1.85}$ is 7.3, 7.8, and 11.1 nm, respectively, which are much smaller than pure CeO_2 (36.2 nm). The substituting process can promote the formation of oxygen vacancies, which can hasten the diffusion rate of oxygen, then improve the combustion activity. According to the catalytic soot combustion results, the ranking in activity of these catalysts is $Ce_{0.7}Zr_{0.3}O_2 > Ce_{0.7}Pr_{0.3}O_{2-\delta} > Ce_{0.7}Gd_{0.3}O_{1.85} \sim CeO_2$, which is well consistent with the reducibility sequence of the samples. The mass of catalyst plus soot mixture have effect on soot combustion: the T_{ig} and T_{max} decrease with the increasing of sample weight. Combustion activity of catalysts decreases slowly with cycled runs, which can be attributed to the activity lost of catalyst.

1. Introduction

Diesel engine vehicles are expected to expand their market in the future because of their better fuel economy compared to gasoline engines. Moreover, they release lower amounts of CO, NO_x, and unburned hydrocarbons [1,2]. However, the emissive soot, an agglomerate of small carbon particles, with different organic compounds adsorbed on their surfaces, forms the major constituents of diesel particulates. These particulates have been considered as a potential carcinogen, which can engender serious human diseases as they can penetrate and lodge within the alveoli of the lung [1,3–6]. These particles range in size between micron level in diameter up to visible soot and have detrimental consequences for the environment either [7].

It appears clear that the reduction of diesel exhaust particulates (DEP) is a challenge in the near future. A way to reduce soot emissions is the use of diesel particulate filter (DPF) placed through the exhaust stream, which has the function to stagnate the soot and to burn it off. To achieve this, the DEP collected in the DPF must be periodically, or continuously, removed from the filter by oxidation. As the soot ignition temperature is usually higher than 550 °C, for spontaneous regeneration under typical engine operating conditions, oxidation catalysts are applied to increase the oxidation rate of soot at lower temperatures [8,9]. Recently a number of catalysts have been reported for the oxidation of DEP, such as noble metal supported catalysts [10–12], and the transition metals oxides (V, Cu, Mn, Cr, Co, Fe, Mo and their mixtures) [2,8,13–16]. As the high cost, the noble metal supported catalysts cannot be employed and extended in the present application. It is also known that eutectic mixtures and low melting point catalysts have superior performances for soot oxidation. The low melting point catalysts, or use of the catalysts in the presence of eutectic salts can increase the soot catalyst contact, therefore increasing the ability of the catalyst to oxidize the soot [17,18]. However, van Setten et al. [19], have recently studied the activity of molten salts, especially Cs_2O, MoO_3, and Cs_2SO_4, and have reported that, despite the promoting activity of these eutectic salts, these coatings are not suitable for application to real systems because their stability is low, then the catalyst compounds would emit into environment and lead to the dramatically drop of oxidation activity.

In CeO_2, the facile Ce^{4+}/Ce^{3+} redox cycle often leads to a higher oxygen-storage capacity with reversible addition and removal of oxygen in the fluorite structure of ceria. The CeO_2 and CeO_2-based solid solutions containing different other rare earth metals were extensively studies for TWC application [20]. Nowadays, a lot of studies are carried out for soot oxidation on CeO_2 [21,22], and CeO_2-based materials [12,23–25] either, especially for $Ce_{1-x}Zr_xO_2$ catalysts [16,26–28], for about 20–40% substitution, the $Ce_{1-x}Zr_xO_2$

* Corresponding author. Fax: +86 579 82282595.
E-mail address: mengfeiluo@zjnu.cn (M.-F. Luo).

0040-6031/$ – see front matter © 2008 Elsevier B.V. All rights reserved.
doi:10.1016/j.tca.2008.08.017

catalysts show the best combustion activity. It was found that CeO_2-based materials have the potential to increase the oxidation rate of soot, because of the high surface area, the creation of "oxygen vacancies" [22,24,29,30], and so on. The generation and feasible utilization of highly reactive "oxygen vacancies" for soot oxidation is the focus of the current studies.

In this study, three cations that own different valences (Zr^{4+}, Pr^{3+}/Pr^{4+} and Gd^{3+}) are chosen to be doped into CeO_2, so the CeO_2-based solid solution catalysts ($Ce_{0.7}Zr_{0.3}O_2$, $Ce_{0.7}Pr_{0.3}O_{2-\delta}$, and $Ce_{0.7}Gd_{0.3}O_{1.85}$) were prepared and tested for activity of soot combustion, and their activities have been compared with pure CeO_2, as well as the influence of the cycled using on the soot combustion. It was hoped that the results might be useful for the development of catalytic removal for diesel soot.

2. Experimental

2.1. Catalysts preparation

$Ce(NO_3)_3{\cdot}6H_2O$ (>99.5%), $Zr(NO_3)_4{\cdot}5H_2O$ (>99.5%), Pr_6O_{11} (>99.95%), Gd_2O_3 (>99.99%), and citric acid (>99.5%) were used as starting materials. All catalysts were prepared by a sol–gel method. For a typical preparation, 2.554 g of Pr_6O_{11} (2.5 mmol) was dissolved in a least amount of dense nitric acid required, then 15.198 g of $Ce(NO_3)_3{\cdot}6H_2O$ (35 mmol) dissolved in 300 ml of deionized water was added to form a Ce–Pr nitrate solution. Citric acid with double molar amount of total metal cations was added to obtain a mixed nitrate and citrate solution. After being stirred for several minutes, the pellucid solution was heated at ca. 90 °C on a magnetic stirrer for several hours until a viscous gel was obtained. The gel was dried at 110 °C overnight, followed by calcination at 600 °C for 4 h in air to obtain the final sample, which was denoted as $Ce_{0.7}Pr_{0.3}O_{2-\delta}$. Thereafter, the $Ce_{0.7}Gd_{0.3}O_{1.85}$, $Ce_{0.7}Zr_{0.3}O_2$, and pure CeO_2 catalysts were prepared in the same way, respectively.

BET-specific surface areas of the catalysts calcined at 600 °C for 4 h was estimated using the N_2 adsorption isotherm at −196 °C by the five points Brunauer–Emmett–Teller (BET) method using an automatic surface analyzer (Quantachrome Autosorb-1-MP instrument).

The simulated soot Printex-U used in this work was industrial flame soot manufactured by Degussa AG, Dusseldorf, Germany. The surface area (BET) of this soot is 96 $m^2\,g^{-1}$, with a mean diameter of 20 nm. It contains approximately 5 wt% of adsorbed hydrocarbons and 0.2–0.4 wt% sulfur [31,32]. The reactive characters of the Printex-U have been determined to be similar to that of actual diesel exhaust soot [33]. Using this soot as a model was initiated by the group at Delft University [8,12,14,23,24,31,32], it is also being commonly used for this purpose by other groups [6,21,22,25,27,28,33–35]. In our experiment, each catalyst and soot in a weight ratio of 9/1, was carefully mixed in an agate mortar to achieve a good contact before it was loaded in the reactor.

2.2. Catalysts characterization

X-ray diffraction (XRD) patterns were collected on a Philips PW 3040/60 powder diffractometer using Cu Kα radiation. The working voltage of the instrument was 40 kV and the current was 40 mA. The intensity data were collected at 25 °C in a 2θ range from 20 to 90° with a scan rate of 1.0° min^{-1} at room temperature. The mean crystallite sizes of catalysts were calculated using the Scherrer equation.

UV-visible diffuse reflectance spectra were obtained on a Thermo Electron spectrophotometer equipped with an integrating sphere.

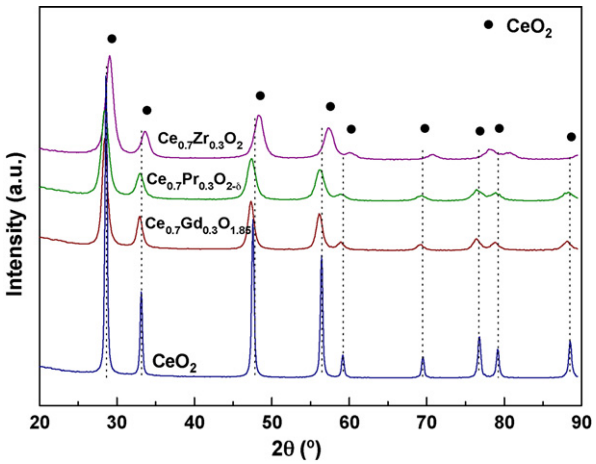

Fig. 1. XRD patterns of CeO_2-based solid solution catalysts calcined at 600 °C.

Raman spectra were obtained with a Renishaw RM 1000 confocal microscope. Room temperature spectra were excited at 514.5 nm line using Ar^+ laser as excitation source. The resolution is ± 1 cm^{-1}. In order to get the comparable data, all samples were pressed to little pellets before their characterization. Data acquisition was carried out at 25 °C with the scanning range from 100 to 1000 cm^{-1}.

The reduction properties of CeO_2-based solid solutions were measured by means of H_2 temperature-programmed reduction (H_2-TPR) technique. 50 mg of sample was placed in a quartz reactor, and the reactor was heated from room temperature to 900 °C at a heating rate of 20 °C min^{-1}. 5% H_2 in N_2 was used as reducing agent with a flow rate of 25 ml min^{-1}. The amount of consumed H_2 during the reduction was calculated based on the analysis with a thermal conductivity detector (TCD).

2.3. Catalytic activity tests

The TPO measurements were performed with a Balzers Omnistar 200 mass spectrometer, monitoring the *m/e* ratios 44 (CO_2). 20.0 mg mixture of the catalyst and soot was located in a quartz micro-reactor and heated in air at 50 °C for 0.5 h with an airflow rate of 20 ml min^{-1} as a pretreatment, then cooled down to room temperature by keeping the same flow rate of air. Afterward, the reactor was heated to 700 °C at a heating rate of 10 °C min^{-1} with the same flow rate.

In order to detect any possible change in the catalyst activity after several combustion cycles, 54.0 mg of $Ce_{0.7}Zr_{0.3}O_2$ catalyst was carefully milled with soot (catalyst/soot weight ratio of 9/1) in an agate mortar, and then was used to perform in a TPO run. After the first run the used catalyst was milled with soot in the same mass ratio and carried out in the TPO performance again. These treatments were repeated so as to carry out up to seven cycles.

3. Results and discussion

3.1. Catalysts characterization

3.1.1. Phase analysis of the catalysts

The BET surface areas of the CeO_2, $Ce_{0.7}Gd_{0.3}O_{1.85}$, $Ce_{0.7}Pr_{0.3}O_{2-\delta}$, and $Ce_{0.7}Zr_{0.3}O_2$ are 17.5, 30.4, 58.2 and 37.6 $m^2\,g^{-1}$, respectively.

Fig. 1 shows XRD patterns of ceria-based solid solution catalysts calcined at 600 °C. For the $Ce_{0.7}Zr_{0.3}O_2$, $Ce_{0.7}Pr_{0.3}O_{2-\delta}$, and $Ce_{0.7}Gd_{0.3}O_{1.85}$ catalysts, the diffraction patterns were in good

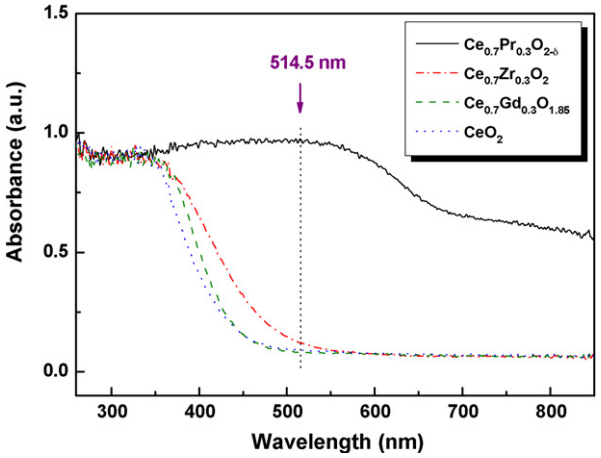

Fig. 2. UV-visible diffuse reflectance spectra of CeO_2-based solid solution catalysts calcined at 600 °C.

agreement with those of pure ceria typical fluorite-like cubic structure (CeO_2, JCPDS: 81-0792), and no diffraction peaks of zirconia, praseodymium oxides, and gadolinium oxides were observed. It confirms that the Zr^{4+}, Pr^{3+}/Pr^{4+}, and Gd^{3+} ions were incorporated into the ceria lattice to form fluorite-like solid solutions. The crystallite size of $Ce_{0.7}Zr_{0.3}O_2$, $Ce_{0.7}Pr_{0.3}O_{2-\delta}$ and $Ce_{0.7}Gd_{0.3}O_{1.85}$ is 7.3, 7.8, and 11.1 nm, respectively. Which are much smaller than that of CeO_2 (36.2 nm). It implies that the formation of CeO_2-solid solutions is favorable to obtain ultrafine nanoparticles.

3.1.2. UV-visible and Raman spectra analysis of catalysts

Fig. 2 presents the UV-visible diffuse reflectance spectra of the CeO_2-based solid solutions catalysts. For $Ce_{0.7}Zr_{0.3}O_2$, $Ce_{0.7}Gd_{0.3}O_{1.85}$, and CeO_2, there are no adsorptions when wavelength is high than 500 nm. However, the $Ce_{0.7}Pr_{0.3}O_{2-\delta}$ catalyst has a strong adsorption at the region of visible light, which may attributed to the color of the $Ce_{0.7}Pr_{0.3}O_{2-\delta}$ (dark brown), as the dark sample can absorb more Raman laser of 514.5 nm than light yellow samples (CeO_2, $Ce_{0.7}Gd_{0.3}O_{1.85}$, and $Ce_{0.7}Zr_{0.3}O_2$).

Fig. 3 shows the Raman spectra of CeO_2-based solid solutions. For all the samples except the $Ce_{0.7}Pr_{0.3}O_{2-\delta}$, there is a feature band at 467 cm^{-1}, which are attributed to the F_{2g} typical vibrational mode of the cubic structure [36,37]. The broad peak around 564 cm^{-1} is attributed to oxygen vacancies generated by the incorporation of other metal cations to the ceria lattice [36,38,39]. These

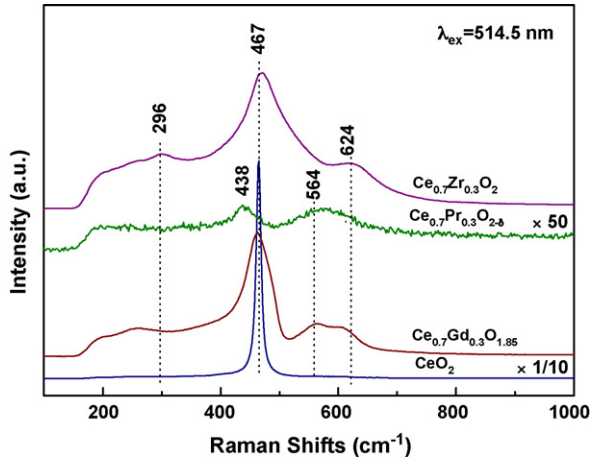

Fig. 3. Laser Raman spectra of CeO_2-based solid solution catalysts calcined at 600 °C.

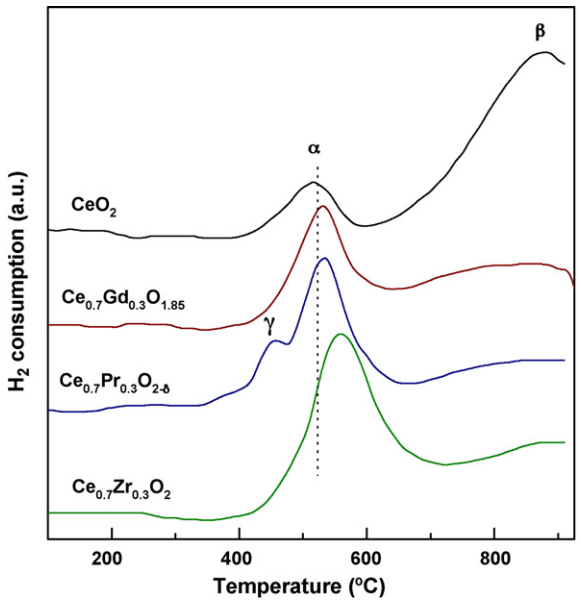

Fig. 4. H_2-TPR profiles of the CeO_2-based solid solutions calcined at 600 °C.

oxygen vacancies can increase the diffusion rate of oxygen and with which the material can absorb and desorb oxygen continuously [36]. For the $Ce_{0.7}Pr_{0.3}O_{2-\delta}$ sample, the Raman bands were much weaker compared to other samples due to its strong absorption of Raman laser at 514.5 nm as shown in Fig. 2. As a number of excitation radiation that enters into the bulk has been absorbed and then the bands supply the information mainly from surface region [39]. Moreover, there is a small systematic shift from the band at 467 cm^{-1} to about 438 cm^{-1}. This shift is attributed the decreasing of the particle sizes at the surface region [40], as Raman band will shift to lower frequencies with the decreasing of crystallite size. The Raman bands at 296 and 624 cm^{-1} were attributed to the tetragonal phase of the solid solutions in the Gd and Zr-doped samples [41,42].

3.1.3. Reduction behavior of the catalysts

Fig. 4 shows the H_2-TPR profiles of the CeO_2-based solid solutions. The single CeO_2 has two reduction peaks at about 517 °C (peak α) and 875 °C (peak β). The peak α was attributed to the reduction at the surface region of CeO_2, and the peak β was attributed to the reduction of the bulk. For the samples $Ce_{0.7}Gd_{0.3}O_{1.85}$, $Ce_{0.7}Pr_{0.3}O_{2-\delta}$ and $Ce_{0.7}Zr_{0.3}O_2$, the temperatures of maximum H_2 consumption peak α is 531, 531 and 560 °C, which slightly shift to higher temperatures, and the peak areas are larger than that of the single ceria. The ratio of main H_2 consumption peak areas for $Ce_{0.7}Zr_{0.3}O_2$:$Ce_{0.7}Pr_{0.3}O_{2-\delta}$:$Ce_{0.7}Gd_{0.3}O_{1.85}$:$CeO_2$ is 4.4:3.1:2.1:1.0. The results suggest that the CeO_2-based solid solutions are more reducible than the pure CeO_2 at the low temperature region (400–700 °C). The reduction peaks at higher temperature (ca. 800 °C) declined significantly, indicating that the reducible sites in the bulk are nearly as active as those at the surface region after forming solid solutions or the reduction temperatures are out of the measurement range.

As praseodymium owns variable valences, for the $Ce_{0.7}Pr_{0.3}O_{2-\delta}$, there is a reduction peak γ at about 456 °C, which could be associated with the reduction of Pr^{4+} to Pr^{3+} at the surface region [43].

3.2. Catalytic activities of catalysts

In the TPO experiments, the main gaseous product detected by mass spectrometry analysis was CO_2 with a trace amount of CO.

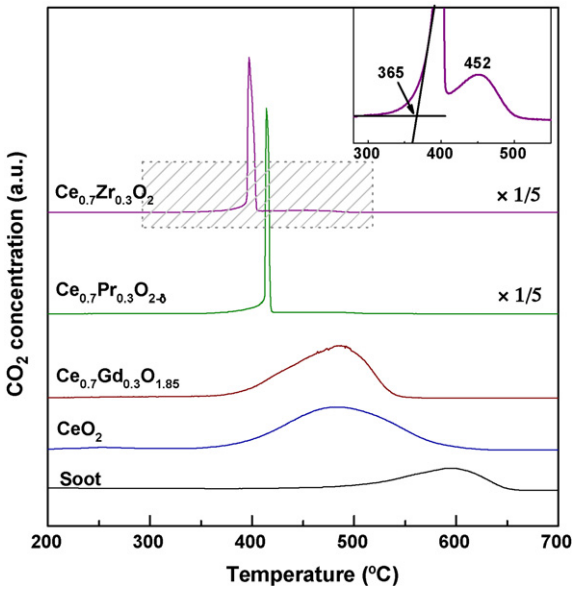

Fig. 5. TPO profiles of CeO_2-based solid solution catalysts mixed with soot (catalyst/soot = 9/1).

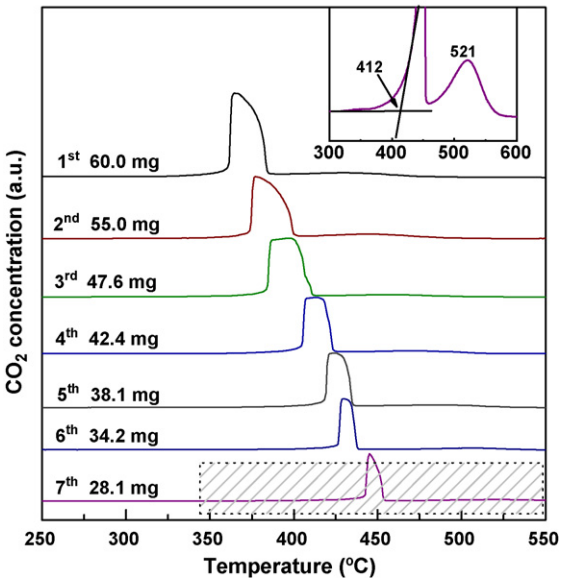

Fig. 6. TPO profiles of combustion cycles over $Ce_{0.7}Zr_{0.3}O_2$ catalyst mixed with soot (catalyst/soot = 9/1).

The formation rate of CO_2 ($m/e = 44$) was used as a measurement to evaluate the catalytic activity. The profiles are shown in Fig. 5, which shows the TPO profiles of CeO_2-based solid solution catalysts mixed with soot. Firstly, the ignition temperature (called T_{ig}) of these mixtures was studied, which was estimated by extrapolating the steeply ascending portion of the carbon dioxide formation curve junction of zero carbon dioxide concentration [44,45]. Table 1 lists the combustion temperatures results of T_{ig}, T_{max} and $\Delta T(T_{max} - T_{ig})$ from TPO tests. It can be seen that the T_{ig} without catalyst (called "soot") is 412 °C. After mixed with catalysts the ignition temperatures decreased, which are attributed to the catalytic combustion of the soot, the T_{ig} for CeO_2 and $Ce_{0.7}Gd_{0.3}O_{1.85}$ are lower than that of $Ce_{0.7}Pr_{0.3}O_{2-\delta}$ and $Ce_{0.7}Zr_{0.3}O_2$.

To compare with literature results, the performance of the catalysts were also evaluated taking the temperature corresponding to the maximum of the peak, called combustion temperature (T_{max}), which represents the temperature of maximum soot combustion. Results show that the T_{max} for soot combustion without catalyst is 594 °C, while T_{max} decreases about 100–200 °C when it was mixed with the catalysts. The $Ce_{0.7}Pr_{0.3}O_{2-\delta}$ and $Ce_{0.7}Zr_{0.3}O_2$ catalysts showed very sharp peaks at 414 and 397 °C. The inset of Fig. 5 amplified from the shadow part of the $Ce_{0.7}Zr_{0.3}O_2$ sample shows a shoulder peak at 452 °C. The area of shoulder peak is about 1/12 of the main peak. Neeft et al. [3,46] concluded that the occurrence of the two peaks was caused by a combination of heat-transport and mass-transport limitation between the $Ce_{0.7}Zr_{0.3}O_2$ and the CO_2 when the mixture is heated. For the $Ce_{0.7}Pr_{0.3}O_{2-\delta}$ sample the shoulder peak is at 465 °C. For the CeO_2 and the $Ce_{0.7}Gd_{0.3}O_{1.85}$ samples the T_{max} is at 485 and 487 °C, respectively, and the peaks are broad, the T_{max} is higher than the shoulder peak (452 and 465 °C), which may be the reason that the shoulder peaks of the CeO_2 and the $Ce_{0.7}Gd_{0.3}O_{1.85}$ cannot be observed. As ΔT represents the difference between T_{max} and T_{ig}, the larger the ΔT is, the lower the activity is. Combined with T_{max} and ΔT in Table 1, the catalytic activities of these samples follow the order: $Ce_{0.7}Zr_{0.3}O_2 > Ce_{0.7}Pr_{0.3}O_{2-\delta} > Ce_{0.7}Gd_{0.3}O_{1.85} \sim CeO_2$.

Table 1
Combustion temperatures results from TPO tests

Samples	T_{ig} (°C)	T_{max} (°C)	$\Delta T(T_{max} - T_{ig})$ (°C)
Soot	412	594	182
Soot + CeO_2	334	485	151
Soot + $Ce_{0.7}Gd_{0.3}O_{1.85}$	344	487	143
Soot + $Ce_{0.7}Pr_{0.3}O_{2-\delta}$	374	414	40
Soot + $Ce_{0.7}Zr_{0.3}O_2$	365	397	32

The catalytic activities of these samples could be influenced by their surface areas, since the CeO_2 with the lowest surface area shows the lowest activity, while the samples with higher surface areas have improved activity. However, it is very likely that the surface area of the sample is not the crucial parameter that determines the overall reactivity. H_2-TPR results (Fig. 4) clearly show that the formation of CeO_2-based solid solutions with small crystallite sizes significantly improve the reducibility of the samples. The order of main H_2 consumption peak areas of the solid solutions is $Ce_{0.7}Zr_{0.3}O_2 > Ce_{0.7}Pr_{0.3}O_{2-\delta} > Ce_{0.7}Gd_{0.3}O_{1.85} > CeO_2$, which is consistent with the order of the catalytic combustion activity. It indicates that the activities of the catalysts could be related to the reducibility of the samples. However, one must keep in mind that the actual mechanism of soot oxidation might be more complex as the combustion peaks on these oxides occur at lower temperatures than those of the corresponding main TPR peaks. Instead, the initial reduction temperature at about 400 °C for these samples well matches the initialization temperature of the corresponding soot oxidation, suggesting that only limited fraction of the overall available oxygen is involved in the reaction, which might be the most facile to be reduced.

The effects of repeated treatments on the activity of these catalysts are important in order to detect any possible change in the catalytic activity after several combustion cycles. A 60.0 mg mixture of $Ce_{0.7}Zr_{0.3}O_2$ and soot (in ratio of 9/1) was performed in the first TPO run. The used catalyst was milled with soot in the same mass ratio again and then carried out in the TPO performance up to seven combustion cycles. Due to the inevitable loss of catalyst during the weighing and milling process, in order to keep the same ratio of catalyst and soot, the mass of mixture gradually decreased in each cycled runs. Fig. 6 shows the TPO profiles of combustion cycles over $Ce_{0.7}Zr_{0.3}O_2$ catalyst mixed with soot. It indicates a changing trend in these profiles: the heavier the mixture mass, the lower the T_{ig} and T_{max} is. Table 2 shows the T_{ig} and T_{max} of $Ce_{0.7}Zr_{0.3}O_2$ catalyst

Table 2
T_{ig} and T_{max} of $Ce_{0.7}Zr_{0.3}O_2$ mixed with soot (catalyst/soot = 9/1) performed in seven combustion cycles (cycled) compared with using different weight (fresh)

Cycled soot + $Ce_{0.7}Zr_{0.3}O_2$			Fresh soot + $Ce_{0.7}Zr_{0.3}O_2$		
Weight (mg)	T_{ig} (°C)	T_{max} (°C)	Weight (mg)	T_{ig} (°C)	T_{max} (°C)
(1st) 60.0	330	365	(1st) 60.0	330	365
(2nd) 55.0	340	377	(2nd) 50.0	333	369
(3rd) 47.6	348	394	(3rd) 45.0	338	373
(4th) 42.4	366	412	(4th) 40.0	339	377
(5th) 38.1	382	424	(5th) 30.0	339	379
(6th) 34.2	393	430	(6th) 25.0	348	381
(7th) 28.1	412	445	(7th) 20.0	365	397

mixed with soot (catalyst/soot = 9/1) performed in seven combustion cycles. After seven TPO runs the mixtures show a shift of the T_{ig} from 330 to 412 °C, and the T_{max} from 365 to 445 °C, meanwhile, from the amplificatory part it shows that the shoulder peak shifted to higher temperature correspondingly. These results indicate that after seven combustion cycles the catalytic activity of $Ce_{0.7}Zr_{0.3}O_2$ decrease gradually. Nevertheless, in the first run the T_{ig} is at 330 °C and T_{max} is 365 °C, which is different from the result in Fig. 5. As in Fig. 5 the 20 mg fresh mixture of $Ce_{0.7}Zr_{0.3}O_2$ and soot shows an obviously higher temperature in both T_{ig} (365 °C) and T_{max} (397 °C). This implies that the mass of the mixture has effect on the combustion process, in order to eliminate the influence of the mass, the effects of the using mass on the catalytic activity need to be studied.

Fig. 7 shows the TPO profiles of $Ce_{0.7}Zr_{0.3}O_2$ catalyst mixed with soot performed using different weight. It can be seen that with the decreasing of mixture weight, the T_{ig} shows a shift from 330 to 365 °C, and the T_{max} from 365 to 397 °C (see Table 2), which indicates that the heavier the mixture mass is, the lower the T_{ig} and T_{max} is. This could be probably associated with the quantity of heat caused by a mass of soot burning which will increase the temperature instantly, and the high temperature environment can help to accelerate the combustion process. Therefore, the combustion temperature enhance with the decreasing of the mixture mass.

In order to verify their hypothesis, TPO experiments of $Ce_{0.7}Zr_{0.3}O_2$ and $Ce_{0.7}Pr_{0.3}O_{2-\delta}$ catalyst mixed with soot or soot + quartz sand (catalyst/soot = 9/1 and catalyst/soot/quartz sand = 9/1/20) were performed (Fig. 8). The catalyst + soot sample (20 mg) diluted in a catalytically inert quartz sand (40 mg) to increase the total solid volume. The result indicates that the T_{max} decrease and the combustion peak become broad after diluted with the quartz sand. It suggests that the dilution with quartz sand facilitates the dissipation of local heat, thus the combustion process become slower. Therefore, the result confirms that the differences found in behavior as a function of catalyst + soot mass is assigned to the generation of hot spots in the mixture.

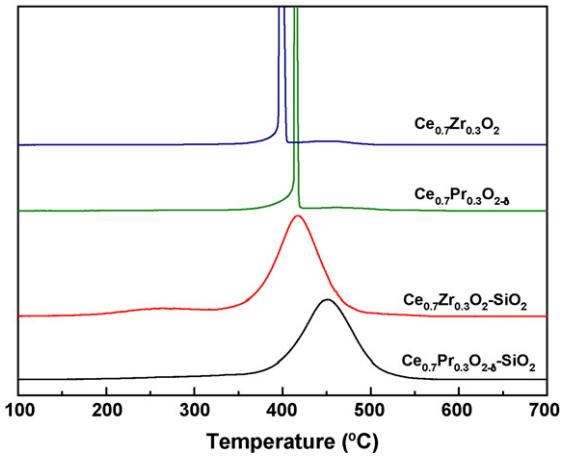

Fig. 8. TPO profiles of $Ce_{0.7}Zr_{0.3}O_2$ and $Ce_{0.7}Pr_{0.3}O_{2-\delta}$ catalyst mixed with soot or soot + quartz sand (catalyst/soot = 9/1 and catalyst/soot/quartz sand = 9/1/20).

In Fig. 7, though the T_{ig} and T_{max} changing trend is similar to that of seven cycled experiment, however, from Fig. 9, the relationship between T_{max} of $Ce_{0.7}Zr_{0.3}O_2$ catalyst mixed with soot performed using different weight (fresh) in comparison with seven combustion cycles, it can be seen that the curve of T_{max} (fresh) are relatively lower than that of T_{max} (cycled), meanwhile, with decreasing mixture weight, the difference in temperature becomes much larger. In fact the difference represents the decrease of combustion catalytic activity, as local heating during combustion cycles may cause sinterization of the used catalyst particles, it would cause a poorer contact with the soot in the consecutive cycles [47]. Therefore, deducing

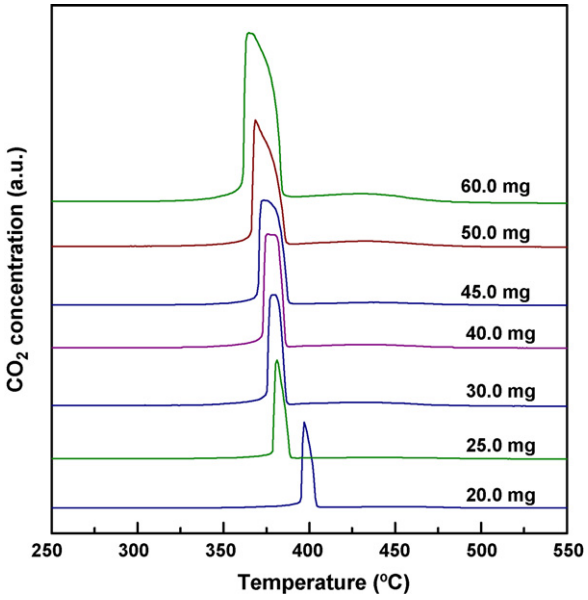

Fig. 7. TPO profiles of $Ce_{0.7}Zr_{0.3}O_2$ catalyst mixed with soot (catalyst/soot = 9/1) performed using different weight.

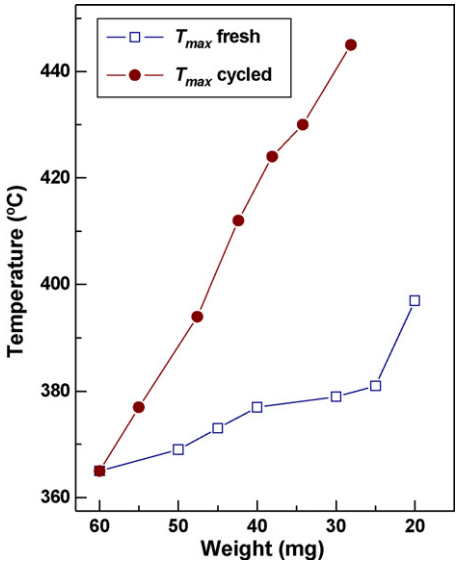

Fig. 9. The relationship between T_{max} of $Ce_{0.7}Zr_{0.3}O_2$ catalyst mixed with soot (catalyst/soot = 9/1) performed using different weight (fresh catalysts) compared with seven combustion cycles (cycled catalysts).

from this effect, it implies that the catalytic activity decrease slowly by cycled using.

4. Conclusions

CeO_2-based catalysts significantly improve the catalytic activity in comparison with pure CeO_2 for soot oxidation by air. As the nanocrystalline solid solution catalysts improve the formation of oxygen vacancies, which can promote the diffusion rate of oxygen, then improve the combustion rate of soot. The best combustion results were obtained with $Ce_{0.7}Zr_{0.3}O_2$ catalyst compared with $Ce_{0.7}Pr_{0.3}O_{2-\delta}$ and $Ce_{0.7}Gd_{0.3}O_{1.85}$. From the cycled running experiment of $Ce_{0.7}Zr_{0.3}O_2$, it indicates that the combustion activity of this catalyst decrease slowly during the repeating using.

Acknowledgments

The support by the Natural Science Foundation of China (Grant 20473075) and the Natural Science Foundation of Zhejiang Province (Z404383) are acknowledged.

References

[1] G. Neri, G. Rizzo, S. Galvagno, A. Donato, M.G. Musolino, R. Pietropaolo, Appl. Catal. B: Environ. 42 (2003) 381–391.
[2] I.C.L. Leocadio, S. Braun, M. Schmal, J. Catal. 223 (2004) 114–121.
[3] J.P.A. Neeft, M. Makkee, J.A. Moulijn, Fuel Process. Technol. 47 (1996) 1–69.
[4] D.W. Dockery, C.A. Pope, X. Xu, J.D. Spengler, J.H. Ware, M.E. Fay, B.G. Ferris, F.E. Speizer, N. Engl. J. Med. 329 (24) (1993) 1753–1759.
[5] Z. Liu, Z. Hao, H. Zhang, Y. Zhuang, J. Chem. Technol. Biotechnol. 77 (2002) 800–804.
[6] N.F. Galdeano, A.L. Carrascull, M.I. Ponzi, I.D. Lick, E.N. Ponzi, Thermochim. Acta. 421 (2004) 117–121.
[7] M. Ambrogio, G. Saracco, V. Specchia, Chem. Eng. Sci. 56 (2001) 1613–1621.
[8] J.P.A. Neeft, M. Makkee, J.A. Moulijn, Appl. Catal. B: Environ. 8 (1996) 57–78.
[9] J.P.A. Neeft, O.P. van Pruissen, M. Makkee, J.A. Moulijn, Appl. Catal. B: Environ. 12 (1997) 21–31.
[10] J.-O. Uchisawa, A. Obuchi, R. Enomoto, S. Liu, T. Nanba, S. Kushiyama, Appl. Catal. B: Environ. 26 (2000) 17–24.
[11] J.-O. Uchisawa, S. Wang, T. Nanba, A. Ohi, A. Obuchi, Appl. Catal. B: Environ. 44 (2003) 207–215.
[12] K. Krishna, A. Bueno-Lopez, M. Makkee, J.A. Moulijn, Appl. Catal. B: Environ. 75 (2007) 201–209.
[13] P. Ciambelli, V. Palma, P. Russo, S. Vaccaro, J. Mol. Catal. A: Chem. 204/205 (2003) 673–681.
[14] J.P.A. Neeft, W. Schipper, G. Mul, M. Makkee, J.A. Moulijn, Appl. Catal. B: Environ. 11 (1997) 365–382.
[15] J.M. Moggia, V.G. Milt, M.A. Ulla, L.M. Cornaglia, Surf. Interface Anal. 35 (2003) 216–225.
[16] E. Aneggi, C. de Leitenburg, G. Dolcetti, A. Trovarelli, Catal. Today 114 (2006) 40–47.
[17] S.J. Jelles, B.A.A.L. van Setten, M. Makkee, J.A. Moulijn, Appl. Catal. B: Environ. 21 (1999) 35–49.
[18] B.A.A.L. van Setten, R. van Dijk, S.J. Jelles, M. Makkee, J.A. Moulijn, Appl. Catal. B: Environ. 21 (1999) 51–61.
[19] B.A.A.L. van Setten, C.G.M. Spitters, J. Bremmer, A.M.M. Mulders, M. Makkee, J.A. Moulijn, Appl. Catal. B: Environ. 42 (2003) 337–347.
[20] W. Wang, P. Lin, Y. Fu, G. Cao, Catal. Lett. 1/2 (2002) 19–27.
[21] I. Atribak, I. Such-Basanez, A. Bueno-Lopez, A. Garcia, J. Catal. 250 (2007) 75–84.
[22] P. Palmisano, N. Russo, P. Fino, D. Fino, C. Badini, Appl. Catal. B: Environ. 69 (2006) 85–92.
[23] A. Bueno-López, K. Krishna, M. Makkee, J.A. Moulijn, J. Catal. 230 (2005) 237–248.
[24] K. Krishna, A. Bueno-Lopez, M. Makkee, J.A. Moulijn, Appl. Catal. B: Environ. 75 (2007) 189–200.
[25] M.A. Malecka, L. Kepinski, W. Mista, Appl. Catal. B: Environ. 74 (2007) 290–298.
[26] Z. Zhang, Y. Zhang, Z. Mu, P. Yu, X. Ni, S. Wang, L. Zheng, Appl. Catal. B: Environ. 76 (2007) 335–347.
[27] J. Liu, Z. Zhao, C. Xu, A. Duan, L. Wang, S. Zhang, Catal. Commun. 8 (2007) 220–224.
[28] E. Aneggi, M. Boaro, C.D. Leitenburg, G. Dolcetti, A. Trovarelli, Catal. Today 112 (2006) 94–98.
[29] S. Rossignol, F. Gérard, D. Mesnard, C. Kappenstein, D. Duprez, J. Mater. Chem. 13 (2003) 3017–3020.
[30] W.H. Weber, K.C. Hass, J.R. McBride, Phys. Rev. B 48 (1) (1993) 178–185.
[31] G. Mul, F. Kapteijn, J.A. Moulijn, Appl. Catal. B: Environ. 12 (1997) 33–47.
[32] J.P.A. Neeft, M. Makkee, J.A. Moulijn, Fuel 77 (3) (1998) 111–119.
[33] H. An, P.J. McGinn, Appl. Catal. B: Environ. 62 (2006) 46–56.
[34] D. Uner, M.K. Demirkol, B. Dernaika, Appl. Catal. B: Environ. 61 (2005) 334–345.
[35] A. Yezerets, N.W. Currier, D.H. Kim, H.A. Eadler, W.S. Epling, C.H.F. Peden, Appl. Catal. B: Environ. 61 (2005) 120–129.
[36] J.R. McBride, K.C. Hass, B.D. Poindexter, W.H. Weber, J. Appl. Phys. 76 (4) (1994) 2435–2441.
[37] M.F. Luo, G.L. Lu, X.M. Zheng, Y.J. Zhong, T.H. Wu, J. Mater. Sci. Lett. 17 (1998) 1553–1557.
[38] Z.Y. Pu, J.Q. Lu, M.F. Luo, Y.L. Xie, J. Phys. Chem. C 111 (2007) 18695–18702.
[39] M.F. Luo, Z.L. Yan, L.Y. Jin, M. He, J. Phys. Chem. B 110 (26) (2006) 13068–13071.
[40] J.E. Spanier, R.D. Robinson, F. Zhang, S.W. Chan, I.P. Herman, Phys. Rev. B 64 (2001) 245407–245414.
[41] D. Kim, H. Jung, I. Yang, J. Am. Ceram. Soc. 76 (1993) 2106–2108.
[42] R. Di Monte, J. Kašpar, J. Mater. Chem. 15 (2005) 633–648.
[43] R. Long, J. Luo, M. Chen, H. Wan, Appl. Catal. A: Gen. 159 (1/2) (1997) 171–185.
[44] W.F. Shangguan, Y. Teraoka, S. Kagawa, Appl. Catal. B: Environ. 16 (1998) 149–154.
[45] W.F. Shangguan, Y. Teraoka, S. Kagawa, Appl. Catal. B: Environ. 12 (1997) 237–247.
[46] J.P.A. Neeft, F. Hoornaert, M. Makkee, J.A. Moulijn, Thermochim. Acta 287 (1996) 261–278.
[47] M. Issa, C. Petit, A. Brillard, J.-F. Brilhac, Fuel 87 (6) (2008) 740–750.